ChemMedChem

Research Article
doi.org/10.1002/cmdc.202300132

Chemistry Europe
European Chemical Societies Publishing

www.chemmedchem.org

Evaluation of the Antiparasitic and Antifungal Activities of Synthetic Piperlongumine-Type Cinnamide Derivatives: Booster Effect by Halogen Substituents

Tariq A. Khan,[a] Ibrahim S. Al Nasr,[b, c] Waleed S. Koko,[c] Jingyi Ma,[d] Simon Eckert,[e] Lucas Brehm,[e] Ridha Ben Said,[f, g] Ismail Daoud,[h, i] Riadh Hanachi,[g] Seyfeddine Rahali,[g] Wendy W. J. van de Sande,[d] Klaus Ersfeld,[e] Rainer Schobert,[j] and Bernhard Biersack*[j]

A series of synthetic *N*-acylpyrrolidone and -piperidone derivatives of the natural alkaloid piperlongumine were prepared and tested for their activities against *Leishmania major* and *Toxoplasma gondii* parasites. Replacement of one of the aryl *meta*-methoxy groups by halogens such as chlorine, bromine and iodine led to distinctly increased antiparasitic activities. For instance, the new bromo- and iodo-substituted compounds **3b/c** and **4b/c** showed strong activity against *L. major* promastigotes (IC_{50} = 4.5–5.8 μM). Their activities against *L. major* amastigotes were moderate. In addition, the new compounds **3b**, **3c**, and **4a–c** exhibited high activity against *T. gondii* parasites (IC_{50} = 2.0–3.5 μM) with considerable selectivities when taking their effects on non-malignant Vero cells into account. Notable antitrypanosomal activity against *Trypanosoma brucei* was also found for **4b**. Antifungal activity against *Madurella mycetomatis* was observed for compound **4c** at higher doses. Quantitative structure-activity relationship (QSAR) studies were carried out, and docking calculations of test compounds bound to tubulin revealed binding differences between the 2-pyrrolidone and 2-piperidone derivatives. Microtubules-destabilizing effects were observed for **4b** in *T. b. brucei* cells.

Introduction

Leishmaniasis is an infectious disease clinically subdivided into visceral leishmaniasis (VL), cutaneous leishmaniasis (CL), and mucocutaneous leishmaniasis (MCL). The CL form causes severe skin lesions, which appear after an infection with various *Leishmania* species such as *L. major*, *L. tropica*, *L. mexicana*, or *L. amazonensis*. It is the most prevalent form of leishmaniasis, with up to one million annual cases, and most of the infected persons are young.[1,2] CL is usually not lethal, but the disfiguring skin lesions are painful and often lead to stigmatizing CL patients.[3,4] The various forms of leishmaniasis are classified as neglected tropical diseases (NTDs) based on a deficiency of available, inexpensive, safe, and efficient treatment options. CL patients are currently treated with pentavalent antimonials, miltefosine, amphotericin B, or pentamidine.[2] In addition to the systemic toxicity of clinically applied drugs such as antimonials, the emergence of drug-resistant parasite forms poses another constantly growing problem. Thus, new potent and cost-effective anti-parasitic drugs against leishmaniasis are needed.

[a] *T. A. Khan*
Department of Clinical Nutrition
College of Applied Health Sciences
Qassim University, Ar Rass 51921 (Saudi Arabia)
[b] *Dr. I. S. Al Nasr*
Department of Biology
College of Science and Arts
Qassim University, Unaizah 51911 (Saudi Arabia)
[c] *Dr. I. S. Al Nasr, Dr. W. S. Koko*
Department of Science Laboratories
College of Science and Arts
Qassim University, Ar Rass 51921 (Saudi Arabia)
[d] *J. Ma, Prof. W. W. J. van de Sande*
Department of Medical Microbiology and Infectious Disease
Erasmus MC, University Medical Center Rotterdam
Dr. Molewaterplein 40, 3015 GD Rotterdam (The Netherlands)
[e] *S. Eckert, L. Brehm, Prof. K. Ersfeld*
Department of Genetics, University Bayreuth
Universitätsstrasse 30, 95440 Bayreuth (Germany)
[f] *Dr. R. Ben Said*
Laboratoire de Caractérisations
Applications et Modélisations des Matériaux
Faculté des Sciences de Tunis
Université Tunis El Manar, Tunis (Tunisia)
[g] *Dr. R. Ben Said, Dr. R. Hanachi, Dr. S. Rahali*
Department of Chemistry
College of Science and Arts at Ar Rass
Qassim University, P.O. Box 53, Ar Rass 51921 (Saudi Arabia)
[h] *Dr. I. Daoud*
University Mohamed Khider
Department of Matter Sciences
BP 145 RP, Biskra 07000 (Algeria)
[i] *Dr. I. Daoud*
Laboratory of Natural and Bio-active Substances
Faculty of Science, Tlemcen University
P.O. Box 119, Tlemcen 13000 (Algeria)
[j] *Prof. R. Schobert, Dr. B. Biersack*
Organic Chemistry Laboratory
University Bayreuth
Universitätsstrasse 30, 95440 Bayreuth (Germany)
E-mail: bernhard.biersack@uni-bayreuth.de

Supporting information for this article is available on the WWW under https://doi.org/10.1002/cmdc.202300132

Human African trypanosomiasis (HAT, also called sleeping sickness) is caused by two *Trypanosoma brucei* strains (*T. b. gambiense* and *T. b. rhodesiense*) and threatens millions of people in Central and East Africa. Nitrofuran- and nitroimidazole-based drugs such as nifurtimox and fexinidazole are currently applied for the treatment of HAT.[5,6] However, patients suffering from advanced *rhodesiense*-HAT still need an efficient and less toxic drug than melarsoprol.

Toxoplasmosis is another protozoal parasitic infectious disease with growing incidences worldwide, which is brought about by the protozoal parasite *Toxoplasma gondii*. As immune-compromised people are at risk of severe complications when infected with the globally occurring *T. gondii* parasites, identifying new drugs for toxoplasmosis treatment in such patients is necessary, including drugs derived from medicinal plants.[7]

In addition to protozoal parasites, fungal pathogens can also cause harmful NTDs. Mycetoma (viz."Madura foot") is a crippling and disfiguring NTD caused either by bacteria or by fungi, and occurs in vast tropical and subtropical regions between 30° North and 15° South of the equator all over the world (the so-called"mycetoma belt"), from Southeast Asia, India and the Middle East over Sudan and West Africa to South and Central America.[8] While bacterial mycetoma (actinomycetoma) infections can be cured by treatment with common antibiotics, there is currently no acceptable treatment for patients suffering from fungal mycetoma (viz. eumycetoma) since response rates of available antifungal drugs are rather low.[9] This low treatment response necessitates the amputation of the infected limb.[10] Thus, the identification of new, cost-effective and more efficient antifungal drug candidates for treating eumycetoma and its main causative agent *Madurella mycetomatis* is of the essence.

Natural products from plants are a rich source for the identification and development of new drugs against human infectious diseases caused by protozoa and fungi.[11–14] Natural ingredients of several *Piper* plants exhibited promising activities against various pathogenic protozoal parasites such as *Leishmania*. The amide alkaloids piperine, isolated from black pepper (*Piper nigrum*), and piperlongumine (also called piplartine), isolated from long pepper (*Piper longum*) and other *Piper* species, are prominent examples of antileishmanial compounds from these plants.[15–18] The cinnamide piperlongumine, viz. 5,6-dihydro-1-[(2*E*)-1-oxo-3-(3,4,5-trimethoxyphenyl)-prop-2-enyl]-2(1*H*)-pyridinone, also killed *Schistosoma* worms, inhibited HIF-2 and the growth of cancer cells, and acted as a senolytic agent by killing senescent cells, while there were no reports on an activity against *T. gondii* until now.[19–21] In addition, compounds **1a–d**, which are synthetic cinnamide analogs of piperlongumine, showed anti-inflammatory activities as well as neuroprotective properties by activation of Nrf2 (Figure 1).[22,23] Various natural and synthetic cinnamates have interesting antileishmanial activities. Structurally simple synthetic cinnamic acid esters exhibited distinct antileishmanial properties.[24] Natural bornyl cinnamates isolated from *Valeriana wallichii* showed mitochondrial damage in promastigotes and in vivo activity in mice infected with *L. major*.[25,26] Cinnamates with hydroxy-functionalized isobenzofuranones and 1,2,3-triazoles

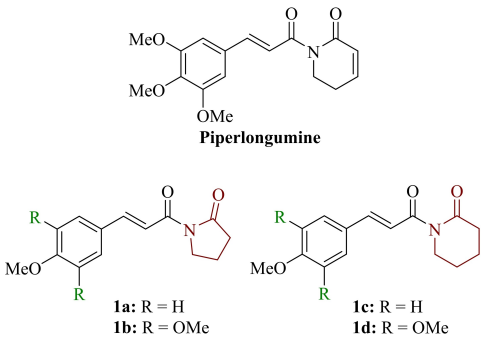

Figure 1. Structures of piperlongumine and the known analogs **1a–d** used in this study.

showed distinct activity against *L. braziliensis* amastigotes originating from apoptosis induction and blocked cytokinesis.[27] Cinnamide conjugates with chloroquine were found active against *L. infantum* promastigotes and amastigotes accompanied by low toxicity.[28] In addition, cinnamic *N*-acylhydrazones were disclosed, which exhibited activity against *L. donovani* amastigotes.[29] *L. amazonensis* arginase was identified as a parasite target for a series of esters and amides of cinnamic acid and caffeic acid derivatives, and selective parasite arginase cinnamides were disclosed.[30,31] In terms of eumycetoma killing cinnamyl derivatives, an oily mixture of cinnamaldehyde with other cinnamoyl and terpenoid derivatives performed especially well, both in vitro and in vivo.[14]

Tubulin is a major drug target in antiparasitic and antifungal research and treatment. Benzimidazoles such as carbendazim, mebendazole and albendazole kill parasites and fungi by disrupting the microtubule structures of treated pathogens.[32] Such benzimidazoles also performed well in *M. mycetomatis* and might become next generation drugs for the treatment of eumycetoma.[33] Piperlongumine and its derivatives were also shown to inhibit tubulin polymerisation rendering this mechanism a reasonable starting point for the design of new cinnamides with detrimental effects on protozoal parasites and pathogenic fungi.[34]

In the present report, we describe a series of new piperlongumine-type cinnamides carrying pyrrolidin-2-one and piperidin-2-one rings and a halogen substitution at one *meta*-position of the phenyl ring. Their activities against *L. major*, *T. gondii*, and *M. mycetomatis* were compared with those of already published analogs such as anisyl- and 3,4,5-trimethoxyphenyl derivatives **1a–d** and with other dihalogenated analogs (Figure 1, Schemes 1 and 2). Docking calculations with tubulin were carried out to evaluate the relevance of tubulin binding for the observed antiparasitic and antifungal activities.

Results and Discussion

The known compounds **1a–d** and **6a** were prepared according to literature procedures.[23,24] Analogously, the new compounds **3a–c**, **4a–c**, **6b–d** and **7a–d** were obtained in moderate yields

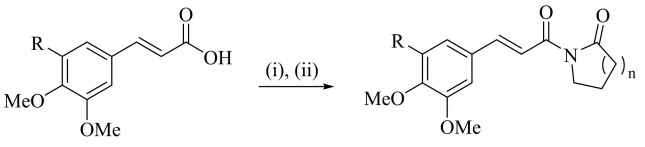

2a: R = Cl
2b: R = Br
2c: R = I

3a: R = Cl, n = 1
3b: R = Br, n = 1
3c: R = I, n = 1
4a: R = Cl, n = 2
4b: R = Br, n = 2
4c: R = I, n = 2

Scheme 1. Reagents and conditions: (i) Oxalyl chloride, cat. DMF, CH_2Cl_2, r.t., 4 h; (ii) 2-pyrrolidone/2-piperidone, Et_3N, CH_2Cl_2, r.t., 24 h, 32–56%.

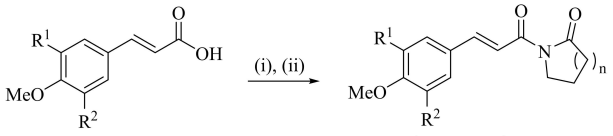

5a: R^1 = OMe, R^2 = H
5b: R^1 = Br, R^2 = H
5c: R^1 = R^2 = Br
5d: R^1 = R^2 = I

6a: R^1 = OMe, R^2 = H, n = 1
6b: R^1 = Br, R^2 = H, n = 1
6c: R^1 = R^2 = Br, n = 1
6d: R^1 = R^2 = I, n = 1
7a: R^1 = OMe, R^2 = H, n = 2
7b: R^1 = Br, R^2 = H, n = 2
7c: R^1 = R^2 = Br, n = 2
7d: R^1 = R^2 = I, n = 2

Scheme 2. Reagents and conditions: (i) Oxalyl chloride, cat. DMF, CH_2Cl_2, r.t., 4 h; (ii) 2-pyrrolidone/2-piperidone, Et_3N, CH_2Cl_2, r.t., 24 h, 30–52%.

Table 1. Cytotoxic concentrations (CC_{50}) of test compounds **1a–d**, **3a–c**, **4a–c**, **6a–d**, and **7a–d** when applied to the Vero (African green monkey kidney epithelial) cell line, and inhibitory concentrations (IC_{50}) when applied to *Toxoplasma gondii* cells.[a] Atovaquone (ATO) was applied against Vero and *T. gondii* as positive control.

Compd	IC_{50} [μM] (*T. gondii*)	CC_{50} [μM] (Vero)	SI (Vero/*T. gondii*)[b]
1a	15.3	30.2	1.97
1b	12.6	18.5	1.47
1c	14.7	28.2	1.92
1d	11.6	18.2	1.57
3a	13.6	22.0	1.62
3b	3.53	13.4	3.80
3c	2.17	23.6	10.9
4a	2.35	39.7	16.9
4b	2.50	32.4	13.0
4c	2.02	26.4	13.0
6a	46.9	45.8	0.98
6b	>40.7	34.6	<0.85
6c	16.4	30.8	1.88
6d	25.0	24.3	0.97
7a	40.8	44.6	1.09
7b	34.6	38.7	1.12
7c	>31.7	>31.7	–
7d	>25.8	>25.8	–
AmB	–	7.7	–
ATO	0.07	9.5	136

[a] Values are the means of at least three independent experiments (SD ± 15%). They were obtained from concentration-response curves by calculating the percentage of treated cells compared to untreated controls after 72 h. [b] Selectivity index SI (CC_{50}/IC_{50}) was calculated from the corresponding IC_{50} values for the Vero cells and the EC_{50} values against *T. gondii*.

from the corresponding cinnamic acids **2a–c** and **5a–d**, which were activated by treatment with oxalyl chloride followed by reaction with 2-pyrrolidone and 2-piperidone, respectively (Schemes 1 and 2). ^{1}H NMR coupling constants of the olefin protons of compounds **3a–c**, **4a–c, 6b–d** and **7a–d** indicate an *E*-configuration of these cinnamide derivatives (J = 15.5–15.8 Hz).

The piperlongumine analogs **1a–d**, **3a–c**, **4a–c**, **6a–d** and **7a–d** were initially tested for their activity against *T. gondii* tachyzoites (Table 1). The known compounds **1a–d** and the new chloro-derivative **3a** displayed only moderate activities against and low selectivities for the *T. gondii* parasites. In contrast, the bromo-derivative **3b** already showed a distinctly higher activity against *T. gondii* and a better selectivity than its close chloro-substituted congener **3a**. The highest activities and selectivities were observed for pyrrolidin-2-one **3c** and the piperidin-2-ones **4a–c**. In addition, these compounds were less toxic than the approved anti-toxoplasmal drug atovaquone (ATO) against the Vero cells. Among them, the iodo-derivatives **3c** and **4c** performed best in terms of activity against *T. gondii* (IC_{50} = 2.0-2.2 μM), which underlines the role of the iodo substituent for an improved anti-parasitic activity. In terms of the chloro-derivatives **3a** and **4a**, it is remarkable that 2-piperidone **4a** was much more active and selective than 2-pyrrolidone **3a**, indicating an important role of the 2-piperidone ring for anti-toxoplasmal activity in this series of anti-parasitic compounds. Compounds **6a–d** and **7a–d** were even less active than compounds **1a–d**, which underlines the importance of the 3-halo-4,5-dimethoxyphenyl scaffold in terms of activity.

The activity of compounds **1a–d**, **3a–c**, **4a–c**, **6a–d**, and **7a–d** against *L. major* promastigotes and amastigotes was also determined (Table 2). Again, compounds **1a–d**, **6a–d**, and **7a–d**, showed only weak activity against both forms of the *L. major* parasite. The presence of bromo- and iodo-substituents led to distinctly higher anti-promastigote activities when compared with the other tested derivatives. The bromo and iodo derivatives **3b/c** and **4b/c** showed the highest activities against *L. major* promastigotes with IC_{50} values between 4.5 and 5.8 μM. In contrast, the chloro derivatives **3a** and **4a** were inactive against the promastigotes, and so were compounds **1a–d**. In addition, compound **4c** was the most active compound against the *L. major* amastigotes albeit it was only moderately active here (IC_{50} = 19 μM). The amastigotes were distinctly less sensitive to cinnamide treatment than the promastigotes. The activities of **3b/c** and **4b/c** are similar to the activities of piperlongumine against promastigotes and amastigotes of other *Leishmania* species.[18] Compared with the positive control, the approved antileishmanial drug amphotericin B (AmB), all tested cinnamides showed lower activities against promastigotes and amastigotes. The test compounds were also investigated for their toxicity to macrophages in order to identify any selectivities for *L. major* parasites. Compounds **4a–c** were less toxic to macrophages than compounds **3a–c**. When compared with their activity against *L. major* promastigotes, compounds **3b**, **3c**, **4b**, and **4c** exhibited a moderate selectivity

Table 2. Inhibitory concentrations (IC_{50}) of test compounds **1a–d**, **3a–c**, **4a–c**, **6a–d**, and **7a–d** when applied to macrophages, promastigotes and amastigotes of *Leishmania major*.[a] Amphotericin B (AmB) was applied as a positive control.

Compd	IC_{50} [μM] promastigotes	IC_{50} [μM] amastigotes	IC_{50} [μM] macrophages
1a	64.4	33.8	64.4
1b	48.5	29.8	38.7
1c	49.0	33.2	66.7
1d	43.5	26.0	46.3
3a	43.9	27.1	25.2
3b	4.52	23.7	24.8
3c	5.73	>31.2	36.9
4a	40.8	25.6	43.9
4b	4.62	>34.0	45.3
4c	5.78	19.0	39.3
6a	36.7	>48.9	>48.0
6b	>40.7	>40.7	>40.7
6c	>32.8	>32.8	>32.8
6d	>26.6	>26.6	>26.6
7a	32.5	>45.6	>45.6
7b	25.7	>39.0	>39.0
7c	>31.7	>31.7	>31.7
7d	>25.8	>25.8	>25.8
AmB	0.83	0.47	–

[a] Values are the means of three experiments (SD ± 15 %). They were obtained from concentration-response curves by calculating the percentage of treated cells compared to untreated controls after 72 h.

for promastigotes with SI values between 5.5 and 9.8 (Table 3). Selectivities for the amastigotes were only marginal (**1c** and **4c** with SI values of 2.0 and 2.1, respectively). Most compounds showed either similar activities, or were more toxic to macrophages.

Compounds **6a–d** and **7a–d** were also inactive against *L. major*, which emphasizes the relevance of the 3-bromo/iodo-4,5-dimethoxyphenyl scaffold for antiparasitic activity.

The promising compounds **3b**, **3c**, **4b**, and **4c** were selected for an evaluation of their activity against *Trypanosoma brucei* parasites, the causative agent of the NTD human African trypanosomiasis (HAT, sleeping sickness), by using the Alamar Blue assay (Table 4). Pentamidine was applied as positive control, while **7b** was added as an inactive example (negative control compound) to this study. First of all, none of the compounds reached the high activity of pentamidine. Compound **4b** was the most active compound against the applied *T. b. brucei* BS442 cells, however, it was less active here than against *T. gondii* and *L. major* promastigotes. Yet, **4b** was more active against *T. b. brucei* than against *L. major* amastigotes. It is noteworthy that the other selected test compounds were distinctly less active against *T. b. brucei* than **4b**, which is in contrast to their performance in *T. gondii* and *L. major* promastigotes.

In addition to their antiparasitic evaluation, compounds **1a–d**, **3a–c**, **4a–c**, **6a–d** and **7a–d** were also tested for their growth inhibitory effects on the fungus *M. mycetomatis*, which is the main causative agent of the human eumycetoma disease (Table 5). The MM55 isolate, which is resistant to cinnamaldehyde (minimal inhibitory concentration/MIC = 222 μg/mL), was used for this study.[14] Although none of the compounds did completely inhibit fungal growth at concentrations of 25 μM and 100 μM, some reduction in growth was observed compared to the solvent-treated control. Compound **4c** demonstrated the highest in vitro activity with percentages metabolic activity of 44.1 % and 26.6 %, respectively. In addition, compounds **3a** and **3c** displayed considerable antifungal activities at 100 μM

Table 3. Selectivity index SI of test compounds was calculated from the corresponding IC_{50} values for the macrophages and the IC_{50} values against *L. major*.

Compd	SI macrophages/promastigotes	SI macrophages/amastigotes
1a	1.0	1.9
1b	0.80	1.3
1c	1.4	2.0
1d	1.1	1.8
3a	0.57	0.93
3b	5.5	1.1
3c	6.4	<1.2
4a	1.1	1.7
4b	9.8	<1.3
4c	6.8	2.1
6a	>1.3	–
7a	>1.4	–
7b	>1.5	–

Table 4. Inhibitory concentrations (IC_{50}) of test compounds **3b**, **3c**, **4b**, **4c**, and **7b** when applied to *T. b. brucei* BS442 cells. Pentamidine was applied as positive control.

Compd	IC_{50} [μM][a]	IC_{50} [μM][b]
3b	56.6 ± 3.1	32.1 ± 0.5
3c	42.1 ± 3.5	26.4 ± 0.4
4b	11.9 ± 1.2	10.5 ± 0.4
4c	25.9 ± 2.8	30.8 ± 0.2
7b	73.71	–
Pentamidine	0.00012 ± 0.0026	–

[a] Values from serial dilution experiments ± SD. [b] Values from linear dilution experiments ± SD.

Table 5. Metabolic activity (in %) upon treatment of *M. mycetomatis* fungi (MM55 isolate) with test compounds **1a–d**, **3a–c**, and **4a–c** at doses of 100 μM and 25 μM. Itraconazole served as positive control.

Compd	100 μM	25 μM
1a	62.9 ± 12.7	56.0 ± 3.6
1b	64.1 ± 24.1	60.7 ± 3.6
1c	47.1 ± 33.5	57.0 ± 6.2
1d	51.7 ± 19.2	46.8 ± 7.0
3a	38.0 ± 1.3	55.2 ± 5.6
3b	52.0 ± 9.1	65.3 ± 26.9
3c	39.9 ± 8.9	56.7 ± 17.1
4a	49.3 ± 17.5	58.7 ± 17.1
4b	58.4 ± 14.1	50.4 ± 9.7
4c	26.6 ± 7.1	44.1 ± 18.5
6a	85.1 ± 19.2	75.0 ± 6.6
6b	77.5 ± 12.6	76.1 ± 8.9
6c	62.9 ± 27.8	66.1 ± 22.7
6d	71.0 ± 15.4	73.0 ± 8.5
7a	63.4 ± 29.4	83.5 ± 7.3
7b	54.6 ± 11.9	64.5 ± 9.8
7c	60.5 ± 20.7	66.1 ± 22.7
7d	67.7 ± 20.2	65.5 ± 5.7
Itraconazole	2.34 ± 4.49[a]	−1.04 ± 2.37[a]

[a] Values taken from Ref. [33].

(38.0% and 39.9% metabolic activity, respectively). Thus, the iodophenyl derivatives **3c** and **4c** performed best in this antifungal assay again, although the reduction in metabolic activity was less than that observed with the positive antifungal control itraconazole. Interestingly, the chloro derivative **3a** was as active as its iodo analog **3c** against *M. mycetomatis*, which is in contrast to their strongly differing activities against the *L. major* promastigotes and the *T. gondii* cells.

In order to establish a rationale for the observed structure-activity relationships, i.e., a mathematical connection between biological activity expressed in terms of pIC_{50} and physicochemical and structural properties of the test compounds, we used a Quantitative Structure-Activity Relationships (QSAR) approach as described previously.[35,36] A good correlation between experimental data and predicted biological activities was obtained for most of the compounds (Figure 2, Table 6).

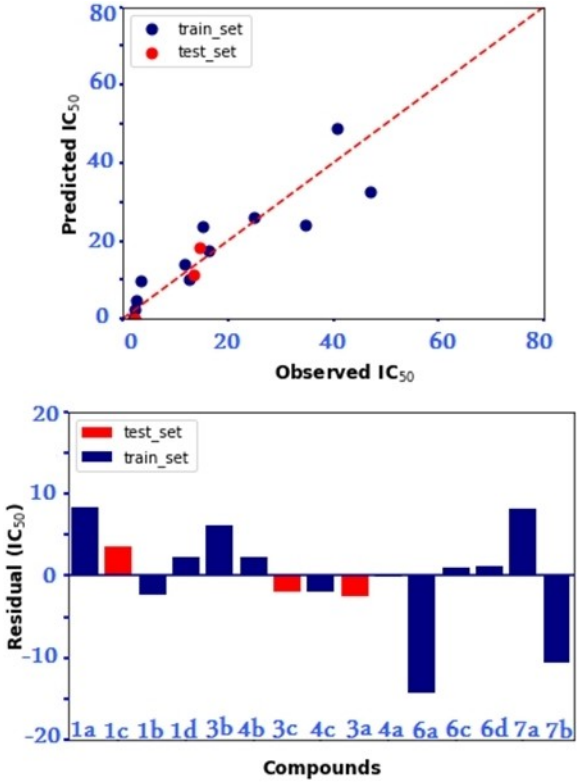

Figure 2. Predicted IC_{50} values of test compounds obtained from the QSAR study and their comparison with observed IC_{50} values.

Both fungal pathogens and protozoal parasites strongly depend on functional cytoskeleton components such as microtubules rendering tubulin a promising target for the design of new antiparasitic and antifungal drug candidates. Thus, docking of test compounds **1a–d**, **3a–c**, and **4a–c** was performed using the PDB structure 1SA0 (Table 7). The structure of colchicine was applied as positive control. The highest affinity was observed for **1d** (score energy = −6.829 kcal/mol), which was slightly lower than the affinity of the known tubulin binder colchicine (score energy = −7.730 kcal/mol). Slightly lower score energies of −6.641 kcal/mol, −6.536 kcal/mol, and −6.615 kcal/mol were calculated for the compounds **1b**, **4a** and **4b**, respectively. Interestingly, 2-piperidone compounds **1d**, **4a** and **4b** interact in a way with the colchicine binding site that is different from the binding modes of colchicine and 2-pyrrolidone **1b** (Figure 3, Table S1). While the trimethoxyphenyl residues of colchicine and **1b** interact strongly with Cys241, this interaction is exerted by the *N*-acrylpiperidone moieties of compounds **1d**, **4a**, and **4b**. Vice versa, the trimethoxy and 3-halo-4,5-dimethoxyphenyl rings of **1d**, **4a** and **4b** formed H-bonds with amino acid residues, which interact with the tropolone and 2-pyrrolidone rings of colchicine or **1b**. The compound couples **3b**/**4b** and **3c**/**4c** similarly differed in their tubulin binding (Figure S5 and S6). In contrast, there were neither distinct tubulin binding differences between the anisyl derivatives **1a** and **1c**, nor between the chloro derivatives **3a** and **4a** (Figures S1, S2, S3, and S4). The anisyl derivatives displayed a unique pi-sulfur interaction with Met259, which was not observed for the other test compounds. Interestingly, Cys241 acted as an H-bond donor only for **3c**, while it was identified as an H-bond acceptor for all other compounds. In most cases, 2-piperidones showed higher binding energies than their 2-pyrrolidone congeners, which can be of relevance for the design of future tubulin binders based on the piperlongumine scaffold.

In order to prove tubulin binding in living parasites, *T. b. brucei* cells were treated with **4b** followed by analysis of the cellular tubulin fractions (insoluble microtubules in the pellets vs. soluble tubulin in the supernatants) via SDS-PAGE

Table 6. Experimental and predicted IC_{50} values of test compounds in *T. gondii* parasites.

Compd	Experimental IC_{50}	Predicted IC_{50}	Residual
1a	15.30	16.62	0.73
1b	12.60	12.60	0
1c	14.70	14.70	0
1d	11.60	11.60	0
3b	5.35	5.35	−1.33
3c	2.17	2.17	0
4a	2.35	2.35	0
4b	2.50	2.50	0
4c	2.02	2.02	0

[a] Values are the means of three experiments (SD ± 15%). They were obtained from concentration-response curves by calculating the percentage of treated cells in comparison to untreated controls after 72 h.

Table 7. S-score energies (in kcal/mol) for the binding of **1a–d**, **3a–c** and **4a–c** to the colchicine binding site of tubulin. The structure of colchicine was used as positive control.)

Compd	S-score [kcal/mol]
1a	−5.852
1b	−6.641
1c	−6.241
1d	−6.829
3a	−5.928
3b	−5.407
3c	−6.047
4a	−6.536
4b	−6.615
4c	−6.071
Colchicine	−7.730

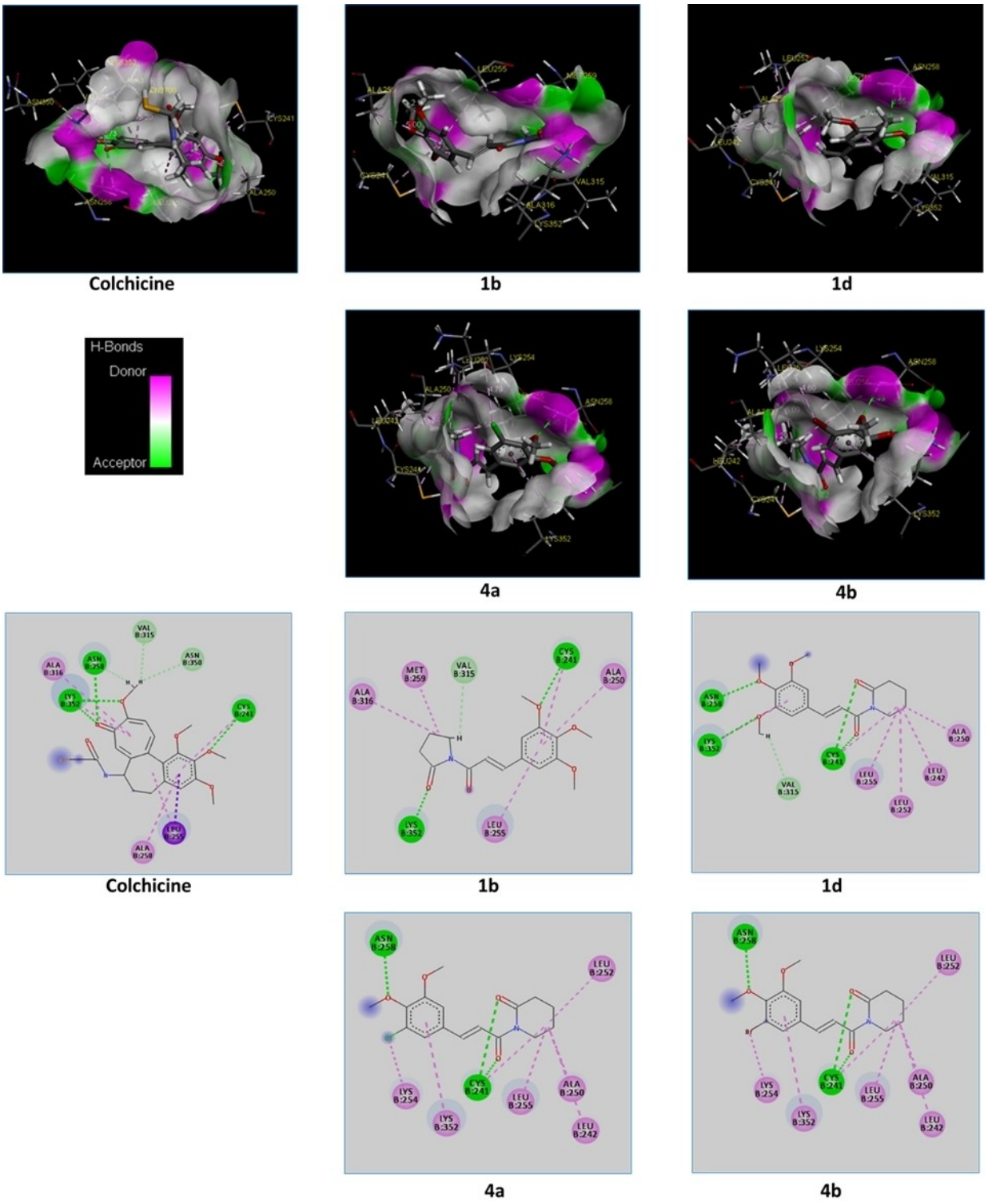

Figure 3. Docking images and interactions of colchicine and compounds **1 b**, **1 d**, **4 a**, and **4 b** when bound to the colchicine binding site of tubulin. Green, H-bond acceptor; purple, H-bond donor.

and Western Blot (Figure 4). Soluble tubulin of *T. brucei* cells in the supernatant increased upon treatment with 10 μM and 50 μM **4 b**, which indicates a dose-dependent tubulin polymerization inhibitory effect by **4 b**.

Conclusions

The evaluation of a series of new cinnamides as drug candidates against pathogenic *T. gondii* and *L. major* parasites revealed distinct dependencies of their activities on the

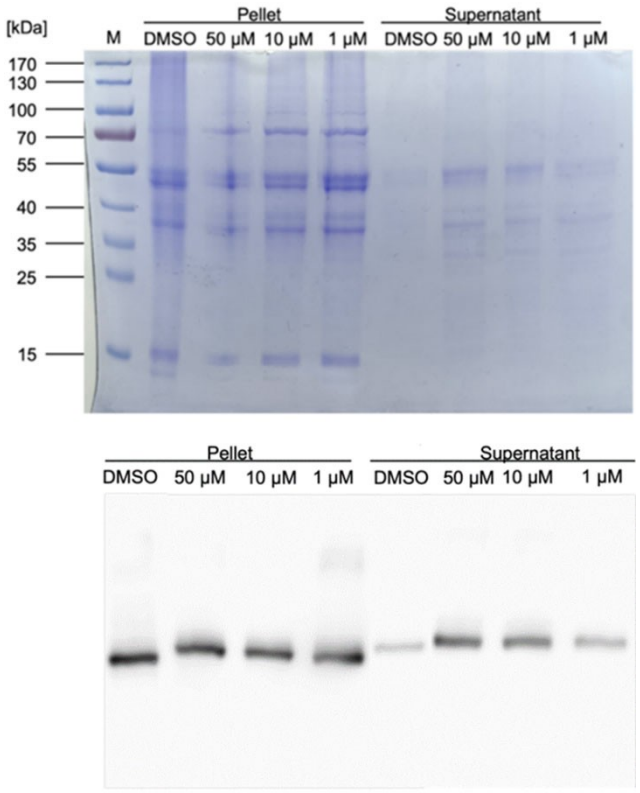

Figure 4. SDS-PAGE (top) and Western Blot (bottom) to detect *T. brucei* tubulin in pellet and supernatant fractions upon treatment of *T. brucei* cells with **4b** (1 µM, 10 µM or 50 µM) for 30 min at room temperature.

presence or absence of a halo-cinnamoyl moiety (Cl, Br, I substituent at one *meta* position of the phenyl ring) and on the nature of the azacycle (2-pyrrolidone or 2-piperidone). Bromo- and iodo-substituted derivatives showed higher antiparasitic activities than their analogs. Antifungal activities against *M. mycetomatis* were only observed for a small number of new derivatives and at much higher concentrations. More detailed research about the mechanisms of action is necessary to identify the reasons for these peculiar effects. Based on the docking results, tubulin is a conceivable target, but its relevance as drug target, and there is evidence for tubulin targeting at least for the 3-bromo-4,5-dimethoxycinnamide **4b** in *T. brucei* cells, may also depend on the investigated parasite. Leishmanial arginase, which was previously identified as a parasitic target for caffeic acid derivatives, is probably not a possible drug target for the cinnamides used in this study as they lack a metal-binding catechol motif. The success of the multimodal drug fexinidazole, which has no specific target, as a ground-breaking oral sleeping sickness therapy can be a blueprint for the development of other presumably pleiotropic agents such as **4b**.

Experimental Section

General

Compounds **1a–d** were prepared following literature procedures and analyzed. The obtained analytical data was in line with published data of these compounds.[23,24] Synthetic procedures and analytical data of the new derivatives are given below. All starting compounds were purchased from the usual providers and used without further purification. Substituted cinnamic acids **2a–c** and **5a–d** were prepared as reported previously.[37,38] Column chromatography: silica gel 60 (230–400 mesh). Melting points (uncorrected), Electrothermal 9100; NMR spectra, Bruker Avance 300 spectrometer; chemical shifts are given in parts per million (δ) downfield from tetramethylsilane as internal standard; Mass spectra, Thermo Finnigan MAT 8500 (EI). Elemental analysis were carried out with an Elementar UNICUBE (Elementar Analysensysteme GmbH).

Chemistry

(E)-1-[3-(3-Chloro-4,5-dimethoxyphenyl)acryloyl]pyrrolidin-2-one (3a) – Typical procedure

3-Chloro-4,5-dimethoxycinnamic acid (100 mg, 0.41 mmol) was dissolved in dry CH_2Cl_2 (3 mL) and oxalyl chloride (218 µL, 2.5 mmol) and two drops of DMF were added. The reaction mixture was stirred at room temperature for 4 h. The solvent was evaporated in vacuum and the residue was dissolved in dry CH_2Cl_2. 2-Pyrrolidone (46 µL, 0.6 mmol) and Et_3N (209 µL, 1.5 mmol) were added and the reaction mixture was stirred at room temperature for 24 h. The reaction mixture was purified by column chromatography (silica gel 60). Yield: 40 mg (0.13 mmol, 32%); off-white solid of m.p. 150 °C; $R_f = 0.58$ (ethyl acetate/*n*-hexane, 1:1); υ_{max}(ATR)/cm^{-1} 3103, 2979, 2943, 1717, 1674, 1623, 1591, 1564, 1494, 1461, 1431, 1412, 1366, 1337, 1307, 1268, 1244, 1202, 1139, 1082, 1050, 1033, 996, 975, 937, 874, 860, 809, 771, 741, 721, 689; ^{1}H NMR (300 MHz, $CDCl_3$) δ 2.0–2.1 (2 H, m, CH_2), 2.6–2.7 (2 H, m, CH_2CO), 3.8–3.9 (8 H, m, CH_2N), 6.99 (1 H, s, Ar–H), 7.21 (1 H, s, Ar–H), 7.65 (1 H, d, $J = 15.7$ Hz, olefin-H), 7.80 (1 H, d, $J = 15.7$ Hz, olefin-H); ^{13}C NMR (75.5 MHz, $CDCl_3$) δ 17.2 (CH_2), 33.9 (CH_2), 45.8 (CH_2N), 56.2 (OCH_3), 60.8 (OCH_3), 110.4 (Ar–CH), 119.4 (olefin-C), 122.5 (Ar–CH), 128.7 (Ar–CCl), 131.3 (Ar–C^q), 143.8 (olefin-C), 147.2 (Ar–C^q), 153.9 (Ar–C^q), 165.9 (CO), 175.7 (CO); *m/z* (%) 311 (52) [M$^+$], 309 (100) [M$^+$], 227 (57), 225 (98), 190 (47); Anal. Calcd. for $C_{15}H_{16}ClNO_4$: C, 58.17; H, 5.21; N, 4.52. Found: C, 58.29; H, 5.13; N, 4.58.

(E)-1-[3-(3-Bromo-4,5-dimethoxyphenyl)acryloyl]pyrrolidin-2-one (3b)

Analogously to the synthesis of **3a**, compound **3b** was obtained from 3-bromo-4,5-dimethoxycinnamic acid (144 mg, 0.5 mmol), oxalyl chloride (218 µL, 2.5 mmol), 2-pyrrolidone (46 µL, 0.6 mmol) and Et_3N (209 µL, 1.5 mmol). Yield: 55 mg (0.16 mmol, 32%); off-white solid of m.p. 164–165 °C; $R_f = 0.40$ (ethyl acetate/*n*-hexane, 1:1); υ_{max}(ATR)/cm^{-1} 3101, 3004, 2979, 2941, 2827, 1716, 1674, 1623, 1590, 1556, 1488, 1460, 1429, 1409, 1365, 1335, 1306, 1264, 1243, 1200, 1137, 1082, 1043, 994, 975, 937, 887, 860, 840, 802, 769, 739, 720, 686; ^{1}H NMR (300 MHz, $CDCl_3$) δ 2.0–2.1 (2 H, m, CH_2), 2.64 (2 H, t, $J = 8.3$ Hz, CH_2CO), 3.8–4.0 (8 H, m, 2 x OCH_3, CH_2N), 7.04 (1 H, s, Ar–H), 7.37 (1 H, s, Ar–H), 7.66 (1 H, d, $J = 15.7$ Hz, olefin-H), 7.81 (1 H, d, $J = 15.7$ Hz, olefin-H); ^{13}C NMR (75.5 MHz, DMSO-d_6) δ 17.2 (CH_2), 33.9 (CH_2), 45.9 (CH_2N), 56.2 (OCH_3), 60.7 (OCH_3), 111.1 (Ar–CH), 118.0 (Ar–CBr), 119.4 (olefin-C), 125.4 (Ar–CH), 132.0 (Ar–C^q), 143.7 (olefin-C), 148.3 (Ar–C^q), 153.7 (Ar–C^q), 165.9 (CO),

175.7 (CO); *m/z* (%) 355 (100) [M^+], 353 (92) [M^+], 271 (72), 269 (73), 190 (96), 175 (19); Anal. Calcd. for $C_{15}H_{16}BrNO_4$: C, 50.87; H, 4.55; N, 3.95. Found: C, 50.78; H, 4.50; N, 4.01.

(E)-1-[3-(3-Iodo-4,5-dimethoxyphenyl)acryloyl]pyrrolidin-2-one (3c)

Analogously to the synthesis of **3a**, compound **3c** was obtained from 3,4-dimethoxy-5-iodocinnamic acid (167 mg, 0.5 mmol), oxalyl chloride (218 μL, 2.5 mmol), 2-pyrrolidone (46 μL, 0.6 mmol) and Et_3N (209 μL, 1.5 mmol). Yield: 66 mg (0.17 mmol, 34%); off-white solid of m.p. 137–139 °C; R_f = 0.43 (ethyl acetate/*n*-hexane, 1:1); υ_{max}(ATR)/cm^{-1} 3104, 2972, 2939, 2835, 1722, 1669, 1620, 1584, 1550, 1481, 1463, 1426, 1407, 1366, 1339, 1305, 1264, 1204, 1141, 1080, 1042, 991, 936, 885, 861, 845, 797, 768, 739, 720, 681; ^{1}H NMR (300 MHz, $CDCl_3$) δ 2.0–2.1 (2 H, m, CH_2), 2.6–2.7 (2 H, m, CH_2CO), 3.83 (3 H, s, OCH_3), 3.87 (3 H, s, OCH_3), 3.9–4.0 (2 H, m, CH_2N), 7.06 (1 H, s, Ar–H), 7.57 (1 H, s, Ar–H), 7.64 (1 H, d, *J* = 15.7 Hz, olefin-H), 7.79 (1 H, d, *J* = 15.7 Hz, olefin-H); ^{13}C NMR (75.5 MHz, $CDCl_3$) δ 17.2 (CH_2), 33.9 (CH_2), 45.9 (CH_2N), 56.0 (OCH_3), 60.5 (OCH_3), 92.6 (Ar–Cl), 112.1 (Ar–CH), 119.2 (olefin-C), 131.3 (Ar–CH), 132.9 (Ar–C^q), 143.5 (olefin-C), 150.8 (Ar–C^q), 152.6 (Ar–C^q), 169.9 (CO), 175.7 (CO); *m/z* (%) 401 (100) [M^+], 317 (54), 175 (33), 76 (28), 41 (27); Anal. Calcd. for $C_{15}H_{16}INO_4$: C, 44.91; H, 4.02; N, 3.49. Found: C, 44.83; H, 3.97; N, 3.53.

(E)-1-[3-(3-Chloro-4,5-dimethoxyphenyl)acryloyl]piperidin-2-one (4a)

Analogously to the synthesis of **3a**, compound **4a** was obtained from 3-chloro-4,5-dimethoxycinnamic acid (100 mg, 0.41 mmol), oxalyl chloride (218 μL, 2.5 mmol), 2-piperidone (60 mg, 0.6 mmol) and Et_3N (209 μL, 1.5 mmol). Yield: 70 mg (0.22 mmol, 54%); off-white solid of m.p. 107–109 °C; R_f = 0.59 (ethyl acetate/*n*-hexane, 1:1); υ_{max}(ATR)/cm^{-1} 3011, 2943, 2879, 1672, 1620, 1563, 1493, 1462, 1446, 1409, 1398, 1346, 1333, 1310, 1298, 1265, 1239, 1198, 1182, 1161, 1139, 1097, 1052, 1022, 1000, 974, 916, 890, 863, 838, 801, 767, 724, 656; ^{1}H NMR (300 MHz, $CDCl_3$) δ 1.8–1.9 (4 H, m, 2xCH_2), 2.5–2.6 (2 H, m, CH_2CO), 3.7–3.8 (2 H, m, CH_2N), 3.85 (3 H, s, OCH_3), 3.86 (3 H, s, OCH_3), 6.95 (1 H, s, Ar–H), 7.17 (1 H, s, Ar–H), 7.31 (1 H, d, *J* = 15.6 Hz, olefin-H), 7.53 (1 H, d, *J* = 15.6 Hz, olefin-H); ^{13}C NMR (75.5 MHz, $CDCl_3$) δ 20.6 (CH_2), 22.5 (CH_2), 34.9 (CH_2), 44.6 (CH_2N), 56.1 (OCH_3), 60.8 (OCH_3), 110.3 (Ar–CH), 122.1 (Ar–CH), 122.5 (olefin-C), 128.6 (Ar–CCl), 131.6 (Ar–C^q), 141.5 (olefin-C), 146.9 (Ar–C^q), 153.8 (Ar–C^q), 169.3 (CO), 173.9 (CO); *m/z* (%) 325 (37) [M^+], 323 (97) [M^+], 295 (24), 280 (20), 225 (100), 190 (47), 98 (15); Anal. Calcd. for $C_{16}H_{18}ClNO_4$: C, 59.36; H, 5.60; N, 4.33. Found: C, 59.27; H, 5.54; N, 4.40.

(E)-1-[3-(3-Bromo-4,5-dimethoxyphenyl)acryloyl]piperidin-2-one (4b)

Analogously to the synthesis of **3a**, compound **4b** was obtained from 3-bromo-4,5-dimethoxycinnamic acid (144 mg, 0.5 mmol), oxalyl chloride (218 μL, 2.5 mmol), 2-piperidone (60 mg, 0.6 mmol) and Et_3N (209 μL, 1.5 mmol). Yield: 98 mg (0.27 mmol, 54%); off-white solid of m.p. 98–100 °C; R_f = 0.48 (ethyl acetate/*n*-hexane, 1:1); υ_{max}(ATR)/cm^{-1} 3014, 2966, 2940, 2896, 2870, 2833, 1687, 1670, 1616, 1588, 1550, 1486, 1448, 1429, 1407, 1387, 1336, 1286, 1269, 1211, 1155, 1109, 1048, 1019, 990, 915, 885, 854, 838, 820, 803, 764, 737, 720, 660; ^{1}H NMR (300 MHz, $CDCl_3$) δ 1.8–1.9 (4 H, m, 2 x CH_2), 2.5–2.6 (2 H, m, CH_2CO), 3.7–3.8 (2 H, m, CH_2N), 3.85 (3 H, s, OCH_3), 3.86 (3 H, s, OCH_3), 6.99 (1 H, s, Ar–H), 7.3–7.4 (2 H, m, Ar–H, olefin-H), 7.53 (1 H, d, *J* = 15.6 Hz, olefin-H); ^{13}C NMR (75.5 MHz, DMSO-d_6) δ 20.6 (CH_2), 22.5 (CH_2), 34.9 (CH_2), 44.6 (CH_2N), 56.1 (OCH_3), 60.7 (OCH_3), 111.0 (Ar–CH), 118.0 (Ar–CBr), 122.5 (olefin-C), 125.0 (Ar–CH), 132.3 (Ar–C^q), 141.4 (olefin-C), 148.0 (Ar–C^q), 153.7 (Ar–C^q), 169.3 (CO), 173.9 (CO); *m/z* (%) 369 (100) [M^+], 367 (98) [M^+], 341 (30), 339 (31), 326 (22), 324 (24), 271 (82), 269 (82), 190 (87), 175 (21); Anal. Calcd. for $C_{16}H_{18}BrNO_4$: C, 52.19; H, 4.93; N, 3.80. Found: C, 52.25; H, 4.90; N, 3.72.

(E)-1-[3-(3-Iodo-4,5-dimethoxyphenyl)acryloyl]piperidin-2-one (4c)

Analogously to the synthesis of **3a**, compound **4c** was obtained from 3,4-dimethoxy-5-iodocinnamic acid (167 mg, 0.5 mmol), oxalyl chloride (218 μL, 2.5 mmol), 2-piperidone (60 mg, 0.6 mmol) and Et_3N (209 μL, 1.5 mmol). Yield: 118 mg (0.28 mmol, 56%); off-white solid of m.p. 97–99 °C; R_f = 0.45 (ethyl acetate/*n*-hexane, 1:1); υ_{max}-(ATR)/cm^{-1} 3018, 2962, 2932, 2892, 2868, 2832, 1686, 1669, 1614, 1583, 1543, 1481, 1448, 1427, 1406, 1387, 1332, 1286, 1266, 1206, 1194, 1174, 1155, 1145, 1109, 1096, 1046, 1018, 991, 914, 888, 855, 840, 811, 794, 759, 719, 656; ^{1}H NMR (300 MHz, $CDCl_3$) δ 1.8–1.9 (4 H, m, 2xCH_2), 2.5–2.6 (2 H, m, CH_2CO), 3.7–3.8 (2 H, m, CH_2N), 3.81 (3 H, s, OCH_3), 3.84 (3 H, s, OCH_3), 7.00 (1 H, s, Ar–H), 7.29 (1 H, d, *J* = 15.6 Hz, olefin-H), 7.4–7.5 (2 H, m, Ar–H, olefin-H); ^{13}C NMR (75.5 MHz, $CDCl_3$) δ 20.5 (CH_2), 22.5 (CH_2), 34.9 (CH_2), 44.6 (CH_2N), 56.0 (OCH_3), 60.5 (OCH_3), 92.6 (Ar–Cl), 112.1 (Ar–CH), 122.3 (olefin-C), 130.8 (Ar–CH), 133.1 (Ar–C^q), 141.2 (olefin-C), 150.4 (Ar–C^q), 152.5 (Ar–C^q), 169.2 (CO), 173.8 (CO); *m/z* (%) 415 (100) [M^+], 387 (17), 372 (15), 317 (65), 190 (57), 175 (22); Anal. Calcd. for $C_{16}H_{18}INO_4$: C, 46.28; H, 4.37; N, 3.37. Found: C, 46.35; H, 4.44; N, 3.41.

(E)-1-[3-(3-Bromo-4-methoxyphenyl)acryloyl]pyrrolidin-2-one (6b)

Analogously to the synthesis of **3a**, compound **6b** was obtained from 3-bromo-4-methoxycinnamic acid (128 mg, 0.5 mmol), oxalyl chloride (218 μL, 2.5 mmol), 2-pyrrolidone (46 μL, 0.6 mmol) and Et_3N (209 μL, 1.5 mmol). Yield: 53 mg (0.16 mmol, 32%); off-white solid of m.p. 207–208 °C; R_f = 0.38 (ethyl acetate/*n*-hexane, 1:1); υ_{max}(ATR)/cm^{-1} 3097, 3061, 2972, 2952, 2910, 2854, 1737, 1666, 1616, 1593, 1554, 1501, 1456, 1444, 1399, 1363, 1332, 1286, 1263, 1243, 1207, 1183, 1155, 1080, 1053, 1033, 1016, 993, 938, 902, 865, 841, 812, 735, 704, 671; ^{1}H NMR (300 MHz, $CDCl_3$) δ 2.0–2.1 (2 H, m, CH_2), 2.6–2.7 (2 H, m, CH_2CO), 3.8–3.9 (5 H, m, CH_2N, OCH_3), 6.86 (1 H, d, *J* = 8.6 Hz, Ar–H), 7.48 (1 H, d, *J* = 8.6 Hz, Ar–H), 7.67 (1 H, d, *J* = 15.7 Hz, olefin-H), 7.7–7.8 (2 H, m, Ar–H, olefin-H); ^{13}C NMR (75.5 MHz, $CDCl_3$) δ 17.1 (CH_2), 33.9 (CH_2), 45.8 (CH_2N), 56.3 (OCH_3), 111.7 (Ar–CH), 112.2 (Ar–CBr), 117.8 (olefin-C), 129.0 (Ar–CH), 129.3 (Ar–C^q), 133.0 (Ar–CH), 143.6 (olefin-C), 157.4 (Ar–C^q), 166.1 (CO), 175.7 (CO); *m/z* (%) 325 (33) [M^+], 323 (32) [M^+], 241 (61), 239 (62), 160 (100), 132 (27), 89 (40); Anal. Calcd. for $C_{14}H_{15}BrNO_3$: C, 51.87; H, 4.35; N, 4.32. Found: C, 51.66; H, 4.40; N, 4.28.

(E)-1-[3-(3,5-Dibromo-4-methoxyphenyl)acryloyl]pyrrolidin-2-one (6c)

Analogously to the synthesis of **3a**, compound **6c** was obtained from 3,5-dibromo-4-methoxycinnamic acid (168 mg, 0.5 mmol), oxalyl chloride (218 μL, 2.5 mmol), 2-pyrrolidone (46 μL, 0.6 mmol) and Et_3N (209 μL, 1.5 mmol). Yield: 61 mg (0.15 mmol, 30%); colorless solid of m.p. 166–167 °C; R_f = 0.37 (ethyl acetate/*n*-hexane, 1:1); υ_{max}(ATR)/cm^{-1} 3093, 3057, 2973, 2933, 2903, 1729, 1669, 1621, 1535, 1472, 1421, 1392, 1361, 1332, 1256, 1216, 1191, 1081, 1066, 1029, 979, 934, 857, 810, 764, 742, 714, 677; ^{1}H NMR (300 MHz, $CDCl_3$) δ 2.0–2.1 (2 H, m, CH_2), 2.6–2.7 (2 H, m, CH_2CO), 3.8–3.9 (5 H, m, CH_2N, OCH_3), 7.59 (1 H, d, *J* = 15.8 Hz, olefin-H), 7.70 (2 H, s, 2 x Ar–H), 7.79 (1 H, d, *J* = 15.8 Hz, olefin-H); ^{13}C NMR (75.5 MHz, $CDCl_3$)

δ 17.2 (CH_2), 33.8 (CH_2), 45.8 (CH_2N), 60.7 (OCH_3), 118.6 (Ar–CBr), 120.7 (olefin-C), 132.3 (Ar–CH), 133.6 (Ar–C^q), 141.6 (olefin-C), 155.4 (Ar–C^q), 165.5 (CO), 175.7 (CO); *m/z* (%) 405 (32) [M^+], 403 (71) [M^+], 401 (32) [M^+], 321 (47), 319 (100), 317 (49), 240 (68), 238 (73), 169 (25), 167 828), 116 (32), 84 (65); Anal. Calcd. for $C_{14}H_{13}Br_2NO_3$: C, 41.72; H, 3.25; N, 3.48. Found: C, 41.78; H, 3.21; N, 3.43.

(E)-1-[3-(3,5-Diiodo −4-methoxyphenyl)acryloyl]pyrrolidin-2-one (6 d)

Analogously to the synthesis of **3 a**, compound **6 d** was obtained from 3,5-diiodo-4-methoxycinnamic acid (137 mg, 0.32 mmol), oxalyl chloride (139 μL, 0.64 mmol), 2-pyrrolidone (29 μL, 0.38 mmol) and Et_3N (133 μL, 0.96 mmol). Yield: 50 mg (0.10 mmol, 31 %); colorless solid of m.p. 179–180 °C; R_f = 0.45 (ethyl acetate/*n*-hexane, 1 : 2); υ_{max}(ATR)/cm^{-1} 3101, 3057, 3029, 2942, 207, 2851, 1728, 1667, 1611, 1521, 1479, 1462, 1413, 1393, 1362, 1340, 1255, 1224, 1082, 1057, 1032, 1009, 986, 935, 917, 887, 765, 707, 677; ^{1}H NMR (300 MHz, $CDCl_3$) δ 2.0–2.1 (2 H, m, CH_2), 2.6–2.7 (2 H, m, CH_2CO), 3.85 (3 H, s, OCH_3), 3.89 (2 H, t, *J* = 7.1 Hz, CH_2N), 7.56 (1 H, d, *J* = 15.7 Hz, olefin-H), 7.78 (1 H, d, *J* = 15.7 Hz, olefin-H), 7.95 (2 H, s, 2 x Ar–H); ^{13}C NMR (75.5 MHz, $CDCl_3$) δ 17.2 (CH_2), 33.9 (CH_2), 45.8 (CH_2N), 60.8 (OCH_3), 90.8 (Ar–CI), 120.5 (olefin-C), 134.8 (Ar–C^q), 139.5 (Ar–CH), 141.3 (olefin-C), 160.3 (Ar–C^q), 165.6 (CO), 175.8 (CO); *m/z* (%) 289 (67) [M^+], 261 (25), 191 (100), 163 (23); Anal. Calcd. for $C_{14}H_{13}I_2NO_3$: C, 33.83; H, 2.64; N, 2.82. Found: C, 33.91; H, 2.70; N, 2.79.

(E)-1-[3-(3,4-Dimethoxyphenyl)acryloyl]piperidin-2-one (7 a)

Analogously to the synthesis of **3 a**, compound **7 a** was obtained from 3,4-dimethoxycinnamic acid (104 mg, 0.5 mmol), oxalyl chloride (218 μL, 2.5 mmol), 2-piperidone (60 mg, 0.6 mmol) and Et_3N (209 μL, 1.5 mmol). Yield: 70 mg (0.24 mmol, 48 %); yellow oil; R_f = 0.32 (ethyl acetate/*n*-hexane, 1 : 1); υ_{max}(ATR)/cm^{-1} 2949, 2838, 2669, 1613, 1594, 1579, 1509, 1462, 1420, 1386, 1341, 1329, 1306, 1291, 1255, 1236, 1194, 1157, 1136, 1105, 1092, 1019, 970, 913, 889, 844, 805, 765, 728; ^{1}H NMR (300 MHz, $CDCl_3$) δ 1.8–1.9 (4 H, m, 2 x CH_2), 2.5–2.6 (2 H, m, CH_2CO), 3.7–3.8 (2 H, m, CH_2N), 3.86 (3 H, s, OCH_3), 3.87 (3 H, s, OCH_3), 6.81 (1 H, d, J = 8.3 Hz, Ar–H), 7.05 (1 H, s, Ar–H), 7.10 (1 H, d, J = 8.3 Hz, Ar–H), 7.31 (1 H, d, J = 15.5 Hz, olefin-H), 7.64 (1 H, d, J = 15.5 Hz, olefin-H); ^{13}C NMR (75.5 MHz, $CDCl_3$) δ 20.5 (CH_2), 22.5 (CH_2), 34.9 (CH_2), 44.5 (CH_2N), 55.8 (OCH_3), 55.9 (OCH_3), 109.8 (Ar–CH), 110.9 (Ar–CH), 119.7 (olefin-CH, 122.8 (Ar–CH), 128.1 (Ar–C^q), 143.5 (olefin-C), 149.0 (Ar–C^q), 150.9 (Ar–C^q), 169.7 (CO), 173.8 (CO); *m/z* (%) 289 (67) [M^+], 261 (25), 191 (100), 163 (23); Anal. Calcd. for $C_{16}H_{19}NO_4$: C, 66.42; H, 6.62; N, 4.84. Found: C, 66.51; H, 6.52; N, 4.75.

(E)-1-(3-Bromo-4-methoxyphenyl)acryloyl)piperidin-2-one (7 b)

Analogously to the synthesis of **3 a**, compound **7 b** was obtained from 3-bromo-4-methoxycinnamic acid (128 mg, 0.5 mmol), oxalyl chloride (218 μL, 2.5 mmol), 2-piperidone (60 mg, 0.6 mmol) and Et_3N (209 μL, 1.5 mmol). Yield: 87 mg (0.26 mmol, 52 %); colorless solid of m.p. 142–143 °C; R_f = 0.46 (ethyl acetate/*n*-hexane, 1 : 1); υ_{max}(ATR)/cm^{-1}2952, 2886, 2844, 1670, 1607, 1592, 1558, 1495, 1476, 1440, 1412, 1390, 1343, 1333, 1294, 1263, 1193, 1174, 1154, 1099, 1083, 1051, 1016, 996, 966, 931, 899, 881, 851, 824, 813, 801, 744, 732, 699, 658; ^{1}H NMR (300 MHz, $CDCl_3$) δ 1.8–1.9 (4 H, m, 2 x CH_2), 2.5–2.6 (2 H, m, CH_2CO), 3.7–3.8 (2 H, m, (CH_2N), 3.88 (3 H, s, OCH_3), 6.83 (1 H, d, *J* = 8.6 Hz, Ar–H), 7.29 (1 H, d, *J* = 15.6 Hz, olefin-H), 7.42 (1 H, d, *J* = 8.6 Hz, Ar–H), 7.56 (1 H, d, *J* = 15.6 Hz, olefin-H), 7.75 (1 H, s, Ar–H); ^{13}C NMR (75.5 MHz, $CDCl_3$) δ 20.6 (CH_2), 22.5 (CH_2), 34.9 (CH_2), 44.6 (CH_2N), 56.3 (OCH_3), 111.7 (Ar–CH), 112.1 (Ar–CBr), 121.0 (olefin-C), 129.2 (Ar–CH), 132.6 (Ar–C^q), 141.4 (olefin-C), 157.1 (Ar–C^q), 169.5 (CO), 173.8 (CO); *m/z* (%) 339 (32) [M^+], 337 (33) [M^+], 311 (15), 309 (15), 214 (70), 239 (70), 160 (100), 132 (33), 89 (47); Anal. Calcd. for $C_{15}H_{16}BrNO_3$: C, 53.27; H, 4.77; N, 4.14. Found: C, 53.33; H, 4.08; N, 4.20.

(E)-1-[3-(3,5-Dibromo-4-methoxyphenyl)acryloyl]piperidin-2-one (7 c)

Analogously to the synthesis of **3 a**, compound **7 c** was obtained from 3,5-dibromo-4-methoxycinnamic acid (168 mg, 0.5 mmol), oxalyl chloride (218 μL, 2.5 mmol), 2-piperidone (60 mg, 0.6 mmol) and Et_3N (209 μL, 1.5 mmol). Yield: 110 mg (0.26 mmol, 52 %); colorless solid of m.p. 162–163 °C; R_f = 0.45 (ethyl acetate/*n*-hexane, 1 : 2); υ_{max}(ATR)/cm^{-1} 29620, 2896, 2882, 1673, 1621, 1534, 1469, 1420, 1390, 1347, 1330, 1294, 1263, 1204, 1178, 1156, 1106, 1093, 1063, 1020, 992, 971, 942, 914, 846, 823, 807, 760, 743, 730, 713, 660; ^{1}H NMR (300 MHz, $CDCl_3$) δ 1.8–1.9 (4 H, m, 2 x CH_2), 2.5–2.6 (2 H, m, CH_2CO), 3.7–3.8 (2 H, m, CH_2N), 3.86 (3 H, s, OCH_3), 7.29 (1 H, d, *J* = 15.6 Hz, olefin-H), 7.45 (1 H, d, *J* = 15.6 Hz, olefin-H), 7.65 (2 H, s, 2 x Ar–H); ^{13}C NMR (75.5 MHz, $CDCl_3$) δ 20.6 (CH_2), 22.5 (CH_2), 34.9 (CH_2), 44.7 (CH_2N), 60.7 (OCH_3), 118.5 (Ar–CBr), 123.8 (olefin-C), 132.0 (Ar–CH), 133.8 (Ar–C^q), 139.1 (olefin-C), 155.1 (Ar–C^q), 168.9 (CO), 173.9 (CO); *m/z* (%) 419 (24) [M^+], 417 (48) [M^+], 415 (26) [M^+], 391 (8), 389 (21), 387 (9), 321 (31), 319 (68), 317 (32), 240 (58), 238 863), 169 (22), 167 (23), 98 (100). Anal. Calcd. for $C_{15}H_{15}Br_2NO_3$: C, 43.19; H, 3.63; N, 3.36. Found: C, 43.08; H, 3.58; N, 3.31.

(E)-1-[3-(3,5-Diiodo-4-methoxyphenyl)acryloyl]piperidin-2-one (7 d)

Analogously to the synthesis of **3 a**, compound **7 d** was obtained from 3,5-diiodo-4-methoxycinnamic acid (137 mg, 0.32 mmol), oxalyl chloride (139 μL, 0.64 mmol), 2-piperidone (38 mg, 0.38 mmol) and Et_3N (133 μL, 0.96 mmol). Yield: 72 mg (0.14 mmol, 44 %); colorless solid of m.p. 198–199 °C; R_f = 0.67 (ethyl acetate/*n*-hexane, 1 : 1); υ_{max}(ATR)/cm^{-1} 2949, 2875, 1671, 1623, 1525, 1459, 1412, 1346, 1327, 1295, 1253, 1203, 1179, 1157, 1105, 1019, 990, 970, 905, 845, 821, 732, 709, 658; ^{1}H NMR (300 MHz, $CDCl_3$) δ 1.8–1.9 (4 H, m, 2 x CH_2), 2.5–2.6 (2 H, m, CH_2CO), 3.7–3.8 (2 H, m, CH_2N), 3.83 (3 H, s, OCH_3), 7.27 (1 H, d, *J* = 15.6 Hz, olefin-H), 7.42 (1 H, d, *J* = 15.6 Hz, olefin-H), 7.90 (2 H, s, 2 x Ar–H); ^{13}C NMR (75.5 MHz, $CDCl_3$) δ 20.6 (CH_2), 22.5 (CH_2), 34.9 (CH_2), 44.7 (CH_2N), 60.8 (OCH_3), 90.8 (Ar–CI), 123.6 (olefin-C), 135.0 (Ar–C^q), 138.8 (Ar–CH), 139.2 (olefin-C), 160.0 (Ar–C^q), 169.0 (CO), 173.9 (CO); *m/z* (%) 511 (97) [M^+], 483 (22), 413 (68), 286 (100), 271 (38), 98 (79); Anal. Calcd. for $C_{15}H_{15}I_2NO_3$: C, 35.25; H, 2.96; N, 2.74. Found: C, 35.32; H, 3.01; N, 2.77.

Toxoplasma gondii cell line, culture conditions, and assay

Serial passages of cells of the Vero cell line (ATCC® CCL81™, USA) were applied for the cultivation of *T. gondii* tachyzoites of the RH strain (a gift from Dr. Saeed El-Ashram, State Key Laboratory for Agrobiotechnology, China Agricultural University, Beijing, China). Vero cells were cultured by using complete RPMI 1640 medium with heat-inactivated 10 % FBS in a humidified 5 % CO_2 atmosphere at 37 °C. 96-Well plates (5×10^3 cells/well in 200 μL RPMI 1640 medium) were used for the cultivation of the Vero cells and then incubated at 37 °C and 5 % CO_2 for one day, followed by removal of medium and washing the cells with PBS. Then, RPMI 1640 medium containing 2 % FBS and *T. gondii* tachyzoites (RH strain) was given to the cells at a ratio of 5 (parasite):1 (Vero cells). After incubation at 37 °C and 5 % CO_2 for 5 h, cells were washed with PBS and then treated as described below. Control: RPMI 1640 medium containing

DMSO (1%) Experimental: Medium + compounds (dissolved in DMSO) (50, 25, 12.5, 6.25, 3.13, 1.65, and 0.75 μg mL^{-1}). After incubation at 37 °C and 5% CO_2 for 72 h, the cells were washed with PBS, fixed in 10% formalin and stained with 1% toluidine blue. Examination of the cells and determination of the infection index (number of cells infected from 200 cells tested) of *T. gondii* were carried out with an inverted photomicroscope. The following equation was used for the calculation of the inhibition in %: Inhibition (%) = (I Control − I Experimental)/(I Control) × 100 where, 'I Control' refers to the infection index of untreated cells and 'I Experimental' refers to the infection index of cells treated with test compounds. Then effects of test compounds on parasite growth were expressed as IC_{50} (inhibitory concentration at 50%) values. IC_{50} values were obtained from three independent experiments.[36,39]

Leishmania major cell isolation, culture conditions, and assays

Promastigotes of *L. major* were isolated from a Saudi patient (February 2016) and maintained at 26 °C in Schneider's Drosophila medium (Invitrogen, USA) containing 10% heat inactivated fetal bovine serum (FBS, Invitrogen, USA) and antibiotics in a tissue culture flask with weekly transfers. Promastigotes were cryopreserved in liquid nitrogen at concentrations of 3×10^6 parasite/mL. Virulent *L. major* parasites were maintained by passing in female BALB/c mice by injecting hind footpads with 1×10^6 stationary-phase promastigotes. *L. major* amastigotes were isolated from the mice after 8 weeks. Isolated amastigotes were converted to promastigotes by cultivation at 26 °C in Schneider's medium supplemented with antibiotics and 10% FBS. Amastigote-derived promastigotes, which had undergone less than five in vitro passages, were used for infection. BALB/c mice (male and female individuals) were obtained from Pharmaceutical College, King Saud University, Kingdom of Saudi Arabia, and maintained in specific pathogen-free facilities. The handling of the laboratory animals followed the instructions and rules of the committee of research ethics, Deanship of Scientific Research, Qassim University, permission number 20-03-20. *L. major* promastigotes from logarithmic-phase were cultured in phenol red-free RPMI 1640 medium (Invitrogen, USA) with 10% FBS and suspended on 96-wells plates to yield 10^6 cells mL^{-1} (200 μL/well) after counting by a hemocytometer. Compounds were added to the wells, obtaining final concentrations of 50, 25, 12.5, 6.25, 3.13, 1.65, and 0.75 μg mL^{-1}. Negative controls contained cultures with DMSO (1%) devoid of test compound and positive control wells contained cultures with decreasing concentrations of amphotericin B (50, 25, 12.5, 6.25, 3.13, 1.65, 0.75 μg mL^{-1}) as active reference compound. After incubation at 26 °C for 72 h, the number of viable promastigotes was assessed by colorimetric method (tetrazolium salt colorimetric assay, MTT). The formed colored formazan was isolated and solubilized by addition of a detergent solution. The samples were analysed by using an ELISA reader at 570 nm. IC_{50} values were calculated from three independent experiments.[36]

For evaluation of the activity against amastigotes in macrophages, peritoneal macrophages were collected from female BALB/c mice (6–8 weeks of age) by aspiration. 5×10^4 cells/well were placed into 96-wells plates containing phenol red-free RPMI 1640 medium with 10% FBS and were incubated to promote cell adhesion at 37 °C for 4 h in 5% CO_2 atmosphere. Thereafter, the medium was discarded and the cells were washed with phosphate buffered saline (PBS). *L. major* promastigotes solution (200 μL at a ratio of 10 promastigotes:1 macrophage in RPMI 1640 medium with 10% FBS) was added to each well and the plates were incubated for 24 h at 37 °C in humidified 5% CO_2 atmosphere to enable macrophage infection and amastigote differentiation. The infected cells were washed three times with PBS to remove the free promastigotes and overlaid with fresh phenol red-free RPMI 1640 medium containing test compounds (50, 25, 12.5, 6.25, 3.13, 1.65, and 0.75 μg mL^{-1}) whereupon the cells were incubated at 37 °C for 72 h in humidified 5% CO_2 atmosphere. Cultures solely containing DMSO (1%) were used as negative controls while wells containing cultures with decreasing concentrations of amphotericin B (reference compound, 50, 25, 12.5, 6.25, 3.13, 1.65, and 0.75 μg mL^{-1}) were used as positive control. The percentage of infected macrophages was evaluated microscopically after the removal of the medium, washing, fixation, and Giemsa staining of the cells. Calculated IC_{50} values were obtained from three independent experiments.[36,40]

In vitro cytotoxicity assay

MTT assays were carried out for a cytotoxicity evaluation of the test compounds. Briefly, both Vero and macrophages cells were cultured in 96-well plates (5×10^3 cells/well/200 μL) for 24 h in RPMI 1640 medium with 10% FBS and 5% CO_2 at 37 °C. Cells were washed with PBS, followed by treatment with test compounds for 72 h at varying concentrations (50, 25, 12.5, 6.25, 3.13, 1.65, and 0.75 μg mL^{-1}) in 10% FBS medium. Cells treated solely with medium in 2% FBS were used as negative control. The supernatant was discarded and 50 μL RPMI 1640 medium containing 14 μL MTT (5 mg mL^{-1}) was added and the cells were incubated for 4 h. The supernatant was removed again and 150 μL DMSO was added in order to dissolve the formed formazan. A FLUOstar OPTIMA spectrophotometer was applied for colorimetric analysis (λ = 540 nm). The cytotoxicity was expressed by CC_{50} values (cytotoxic concentration which caused a 50% reduction in viable cells). CC_{50} values were calculated from three independent experiments.[36,41]

Trypanosoma brucei cell culture conditions and Alamar Blue assay

Cryopreserved trypomastigotes *T. brucei* (BS442) cells were thawed and maintained in HMI-9 cell culture medium containing 10% sterile fetal bovine serum (FBS) in a tissue culture flask at 37 °C with transfers every three days. The cell density was determined, using the Casy TT cell counter (Schärfe System GmbH, Reutlingen, Germany). Alamar Blue® assays were used, for assessing the cytotoxicity of the various test substances on *T. brucei* cells. A stock of 10 mM in dimethyl sulfoxide (DMSO) was prepared for each test compound. From these stocks further dilutions were achieved by diluting the compounds with sterile HMI-9 medium. In total, three dilutions were made: serial doubling dilutions of the compounds with a start concentration of 10 μM or 265 μM, respectively and a linear dilution starting with 73 μM and 3 μM steps per well. With a multichannel pipette, 100 μL of sterile HMI-9 medium was set up in a 96-well plate. The serial doubling dilutions were performed by taking 100 μL from the first well and mixing that with the medium in the following well. A linear change in concentration was achieved by pipetting the amount of stock and medium manually. Finally, three identical dilution series were prepared per 96 well plate with a DMSO control and a blank control. A cell count was performed, and the density adjusted to 8×10^4/mL in full HMI-9/10% FBS. 100 μL of this suspension was then added to all wells (except blank control), and the final concentration was 4×10^4 cells/mL, which corresponds to 4×10^3 cells/well. The plates incubated for 48 h at 37 °C in a CO_2 incubator after which 20 μL of sterile filtered Alamar Blue® solution was added to each well with a multichannel pipette and the plates where incubated for further 12–24 h. Measurement of fluorescence was performed in a fluorescent plate reader at 544 nm excitation and 590 nm emission wavelength. Data was automatically stored and accessed via the application "Omega-Data Analysis". IC_{50} values (represents the

concentration of a test compound that is required for 50% cell death in vivo) were calculated on the website ic50/tk.

In vitro antifungal assay

M. mycetomatis isolate MM55 was used to determine the antifungal activity of each analogue. This fungal isolate was kindly provided by Prof. Ahmed Fahal of the Mycetoma Research Center in Sudan, and maintained in the Erasmus Medical Centre, Rotterdam, The Netherlands. The assay was performed as reported previously.[33] The mycelia were grown at 37 °C in RPMI 1640 medium supplemented with 0.35 g/L L-glutamine and 1.98 mM 4-morpholinepropane sulfonic acid. *M. mycetomatis* mycelia in RPMI 1640 medium were sonicated for 10 s (SoniPrep) and centrifuged at 2600× g for 5 min. The mycelia were washed and resuspended in fresh RPMI 1640 medium to obtain a fungal suspension of 68% to 72% transmission at 660 nm (Novaspec II spectrophotometer). Test compounds were tested at 25 μM and 100 μM in a round-bottom 96-well microtiter plate (Corning, CLS379). Itraconazole was used as positive control at 25 μM and 100 μM. Exactly 100 μL of adjusted fungal suspension was added to each well along with 1 μL of the drug. The plates were sealed and incubated at 37 °C for 7 days. After incubation, 100 μL of XTT work solution (5 mL XTT (Sigma), 1 mg/mL in NaCl; 0.6 mL menadione (Sigma), 1 mM and 4.4 mL in NaCl) was added to each well, followed by incubation at 37 °C for 2 h and at room temperature for 3 h. The extinction of the supernatant was measured at 450 nm in a microplate reader (Epoch2, Biotek, USA). All assays were performed in triplicate.

Cytoskeleton extraction, SDS PAGE and Western Blot analysis

Cytoskeleton extraction and incubation with the test compounds, followed by gel electrophoresis was carried out for a microtubule depolymerization evaluation. A total of 4×10^7 *T. brucei* BS442 cells were centrifuged at 8000 rpm for 5 min per test approach. The supernatant was discarded, and the cells were washed with 200 μL PBS, followed by 3 min centrifugation at 8000 rpm. To separate the cell fractions into soluble and cytoskeleton-associated protein fractions, cells were detergent-extracted. The pellets were resuspended in 200 μL PM buffer (0.1% Tween 20 in PBS, 100 mM PIPES, 1 mM $MgSO_4$, pH^6.9) + 1% (v/v) Nonidet P-40 and incubated on ice for 2 min. The cytoskeletal proteins were separated by a 2-minute centrifugation at 13.300 rpm and the supernatant containing the soluble fraction was removed. After a washing step with 200 μL PM, the pellets were resuspended and incubated with 200 μL of the respective test substance (1 μM, 10 μM, or 50 μM concentrations, diluted in ddH_2O) for 30 min at room temperature. A subsequent centrifugation at 13.300 rpm for 5 min again separated the soluble proteins derived from depolymerization activities of the test compounds and the insoluble pellet fraction. This pellet fraction was washed in 200 μL PM and dissolved in 50 μL SDS sample buffer (10 min, 95 °C). The pellet fractions were finally stored at −20 °C. With the aim to concentrate protein samples derived from the soluble supernatant of the cytoskeleton after treatment with the test compounds, samples were precipitated with TCA. First, only 150 μL supernatant was taken from the sample after incubation with the test substances, to prevent impurities by picking proteins from the pellet fraction. The supernatant fractions were mixed 1:1 with a 20% (w/v) TCA solution and incubated for 30 min on ice. Following a centrifugation step for 10 min at 14.000 rpm and 4 °C, the pellets with precipitated proteins were washed in 500 μL ice-cold 70% ethanol. After a second centrifugation, the pellets were air-dried and dissolved in 50 μL SDS sample buffer. In case of a color change from blue to yellow, indicating TCA residues in the sample, 1 M unbuffered Tris solution was used for back titration. The concentrated sample was boiled (10 min, 95 °C) prior to storage at −20 °C. To separate protein samples by molecular weight and to receive evidence about the quantity of depolymerized proteins, denaturing SDS-PAGE was applied. The acrylamide gel was composed of a focusing gel (6% acrylamide) and a separating gel (8% acrylamide). 5 μL of protein samples were loaded onto the gel and run for 30–40 min at 30 A. As a molecular weight standard, PageRuler Prestained protein ladder (Thermo Fisher Scientific, Waltham, MA), was used. Finally, the gels were stained with Coomassie Brilliant Blue overnight and destained two times in destain solution for 30 min each and in water for 1 h, followed by documentation with a mobile phone camera. For a more detailed analysis, a Western Blot was used after gel electrophoresis. The gel from SDS-PAGE containing 5 μL sample (diluted 1:10 in SDS sample buffer) was applied, using the tank blot method. In a blotting chamber, a filter membrane, Whatman filter paper, the SDS gel with proteins and a polyvinylidene fluoride (PVDF) membrane were assembled and covered with blotting buffer. Blotting was performed at 250 mA for 2 h and successful protein transfer quality was evaluated by Ponceau S staining. To block unspecific binding sites, the membrane was incubated two times in blocking buffer for 15 min. The primary antibody (TAT, mouse anti α-tubulin mAb, diluted 1:10.000 in blocking buffer) was added and incubated overnight, followed by three washing steps with PBS-T for 5 min, respectively. The HRP-conjugated secondary antibody (Peroxidase-conjugated goat anti-mouse IgG, diluted 1:80.000 in blotting buffer) was applied for 2 h. After three subsequent washing steps in PBS-T and PBS, Western Blot Ultra-Sensitive HRP Substrate (Takara BIO INC., Kusatsu, Japan) was added to the membrane, to activate chemiluminescence. The membrane was finally analyzed at an LAS-4000 Imaging System (Fujifilm Europe GmbH, Ratingen, DE).

Computational methods

Validated QSAR models were determined as described previously.[35,36] Molecular docking was performed with MOE version 2014.09.[40] For preparation of the protein and the ligands for docking, the Dock option was used.[42,43] The software source was The Chemical Computing Group Inc., Montreal, QC, Canada. The docking procedure has been described earlier.[44–46] The PDB file –1SA0 was downloaded from the Protein Data Bank for the three dimensional structure of tubulin. First, the 3D Structures of test compounds, **1a–d, 3a–c**, and **4a–c** were built with MOE software, and we minimized them by using the MMFF94x force-field with reaction-field electrostatics (Din = 1, Dout = 80) using a flat bottom tether (10.0 kcal/ mol, 0.25 Å), which was applied to all atoms. Second, the database was created by converting all structures into *.mdb file format in order to use them as input for MOE-docking simulation. The ligands were made flexible and the protein was kept rigid. The water molecules, ions, and cofactors were removed from the PDB structure of target to simplify the simulation; in addition, we kept the chain A of the target for docking experiments. Standard docking procedures for a rigid protein and a flexible ligand were used as per user guide for MOE Software. Briefly, the following default parameters were used: Placement: Triangle Matcher; Rescoring 1: London dG. The London dG scoring function was used to estimate the lowest score energy of the complex with the best poses of test compound. Among the ten poses of the ligands that we obtained, we chose the best binding mode for each ligand, which were visualized using the Discovery Studio 2017 R2 Client software (*Dassault Systèmes BIOVIA, Discovery Studio Modeling Environment*, 2020).

Acknowledgements

We are grateful to Prof. Ahmed Fahal of the Mycetoma Research Center in Sudan for providing M. mycetomatis *strain MM55 for the in vitro antifungal susceptibility testing, and to the College of Applied Health Sciences at Ar Rass, Qassim University. Open Access funding enabled and organized by Projekt DEAL.*

Conflict of Interest

The authors declare no conflict of interest.

Data Availability Statement

The data that support the results of this study are available from the corresponding author upon reasonable request.

Keywords: Piperlongumine · Halogen · Antiparasitic drugs · Mycetoma · Neglected tropical diseases

[1] http://www.who.int/mediacentre/factsheets/fs375/en/, accessed November 12, 2020.
[2] K. van Bocxlaer, D. Caridha, C. Black, B. Vesely, S. Leed, R. J. Sciotti, G.-J. Wijnant, V. Yardley, S. Braillard, C. E. Mowbray, J.-R. Ioset, S. L. Croft, *IJP: Drugs Drug Resist.* **2019**, *11*, 129–138.
[3] I. Bennis, L. Belaid, V. de Brouwere, H. Filali, H. Sahibi, M. Boelart, *PLoS One* **2017**, *12*, e0189906.
[4] M. Kassi, A. Afghan, R. Rehman, P. M. Kasi, *PLoS Neglected Trop. Dis.* **3008**, *2*, e259.
[5] https://dndi.org/diseases/sleeping-sickness/, accessed January 27, 2023.
[6] S. Bernhard, M. Kaiser, C. Burri, P. Mäser, *Diseases* **2022**, *10*, 90.
[7] I. Al Nasr, F. Ahmed, F. Pullishery, S. El-Ashram, V. V. Ramaiah, *Asian Pac. J. Trop. Med.* **2016**, *9*, 730–734.
[8] W. W. J. van de Sande, *PLoS Neglected Trop. Dis.* **2013**, *7*, e2550.
[9] E. E. Zijlstra, W. W. J. van de Sande, O. Welsh, E. S. Mahgoub, M. Goodfellow, A. H. Fahal, *Lancet Infect. Dis.* **2016**, *16*, 100–112.
[10] S. H. Suleiman, E. S. Wadaella, A. H. Fahal, *PLoS Neglected Trop. Dis.* **2016**, *10*, e0004690.
[11] D. Ndjonka, L. N. Rapado, A. M. Silber, E. Liebau, C. Wrenger, *Int. J. Mol. Sci.* **2013**, *14*, 3395–3439.
[12] N. Singh, B. B. Mishra, S. Bajpai, R. K. Singh, V. K. Tiwari, *Bioorg. Med. Chem.* **2014**, *22*, 18–45.
[13] W. S. Koko, I. S. Al Nasr, T. A. Khan, R. Schobert, B. Biersack, *Chem. Biodiversity* **2021**, *18*, e202100542.
[14] M. Konings, K. Eadie, W. Lim, A. H. Fahal, J. Mouton, N. Tesse, W. W. J. van de Sande, *PLoS Neglected Trop. Dis.* **2021**, *15*, e0009488.
[15] J. F. Peixoto, Y. J. Ramos, D. de Lima Moreira, C. R. Alves, L. F. Goncalves-Oliveira, *Parasitol. Res.* **2021**, *120*, 2731–2747.
[16] B. Salehi, Z. A. Zakaria, R. Gyawali, S. A. Ibrahim, J. Rajkovic, Z. K. Shinwari, T. Khan, J. Sharifi-Rad, A. Ozleyen, E. Turkdonmez, M. Valussi, T. Boyunegmez-Tumer, L. M. Fidalgo, M. Martorell, W. N. Setzer, *Molecules* **2019**, *24*, 1364.
[17] P. M. Cheuka, G. Mayoka, P. Mutai, K. Chibale, *Molecules* **2017**, *22*, 58.
[18] J. C. Ticona, P. Bilbao-Ramos, N. Flores, M. A. Dea-Ayuela, F. Bolás-Fernández, I. A. Jiménez, I. L. Bazzocchi, *Food* **2020**, *9*, 1250.
[19] H. R. Bokesch, R. S. Gardella, D. C. Rabe, D. P. Bottaro, W. M. Linehan, J. B. McMahon, T. C. McKee, *Chem. Pharm. Bull.* **2011**, *59*, 1178–1179.
[20] Y. Wang, J. Chang, X. Liu, X. Zhang, S. Zhang, X. Zhang, D. Zhou, G. Zheng, *Aging* **2016**, *8*, 2915–2926.
[21] S. Daley, G. A. Cordell, *Molecules* **2021**, *26*, 3800.
[22] Y. H. Seo, J.-K. Kim, J.-G. Jun, *Bioorg. Med. Chem. Lett.* **2014**, *24*, 5727–5730.
[23] S. Peng, B. Zhang, X. Meng, J. Yao, J. Fang, *J. Med. Chem.* **2015**, *58*, 5242–5255.
[24] F. A. Bernal, M. Kaiser, B. Wünsch, T. J. Schmidt, *ChemMedChem* **2020**, *15*, 68–78.
[25] J. Glaser, M. Schultheis, H. Moll, B. Hazra, U. Holzgrabe, *Molecules* **2015**, *20*, 5740–5753.
[26] A. Masic, A. M. V. Hernandez, S. Hazra, J. Glaser, U. Holzgrabe, B. Hazra, U. Schurigt, *PLoS One* **2015**, *10*, e0142386.
[27] M. P. Rodrigues, D. C. Tomaz, L. A. de Souza, T. S. Onofre, W. A. de Menezes, J. Almeida-Silva, A. M. Suarez-Fontes, M. R. de Almeida, A. M. da Silva, G. C. Bressan, M. A. Vannier-Santos, J. L. R. Fietto, R. R. Teixeira, *Eur. J. Med. Chem.* **2019**, *183*, 111688.
[28] S. Vale-Costa, J. Costa-Gouvela, B. Pérez, T. Silva, C. Teixeira, P. Gomes, M. S. Gomes, *Antimicrob. Agents Chemother.* **2013**, *57*, 5112–5115.
[29] S. A. Carvalho, M. Kaiser, R. Brun, E. F. da Silva, C. A. M. Fraga, *Molecules* **2014**, *19*, 20374–20381.
[30] E. R. da Silva, S. Brogi, A. Grillo, G. Campiani, S. Gemma, P. C. Vieira, C. do Carmo Maquiaveli, *Chem. Biol. Drug Des.* **2019**, *93*, 139–146.
[31] E. R. da Silva, J. A. A. dos Santos Simone Come, S. Brogi, V. Calderone, G. Chemi, G. Campiani, T. M. F. da Sousa Oliveira, T.-N. Pham, M. Pudlo, C. Girard, C. do Carmo Maquiaveli, *Molecules* **2020**, *25*, 5271.
[32] E. Lacey, *Parasitol. Today* **1990**, *6*, 112–115.
[33] W. Lim, B. Nyuykonge, K. Eadie, M. Konings, J. Smeets, A. Fahal, A. Bonifaz, M. Todd, B. Perry, K. Samby, J. Burrows, A. Verbon, W. van de Sande, *PLoS Neglected Trop. Dis.* **2022**, *16*, e0010159.
[34] M. J. Meegan, S. Nathwani, B. Twamley, D. M. Zisterer, N. M. O'Boyle, *Eur. J. Med. Chem.* **2017**, *125*, 453–463.
[35] M. Ghamri, D. Harkati, S. Belaidi, S. Boudergua, R. Ben Said, R. Linguerri, C. Chambaud, M. Hochlaf, *Spectrochim. Acta A: Biomol. Spectr.* **2020**, *242*, 118724.
[36] I. S. Al Nasr, R. Hanachi, R. B. Said, S. Rahali, B. Tangour, S. I. Abdelwahab, A. Farasani, M. M. E. Taha, A. Bidwai, W. S. Koko, T. A. Khan, R. Schobert, B. Biersack, *Bioorg. Chem.* **2021**, *114*, 105099.
[37] V. A. Kumari, K. Bharathi, K. Prabhu, K. Ponnudurai, *Asian J. Chem.* **2016**, *28*, 1895–1898.
[38] F. B. Wittmer, L. C. Raiford, *J. Org. Chem.* **1945**, *10*, 527–532.
[39] H. Jelali, I. Al Nasr, W. Koko, T. Khan, E. Deniau, M. Sauthier, F. Alresheedi, N. Hamdi, *J. Heterocycl. Chem.* **2022**, *59*, 493–506.
[40] E. Osorio, G. Arango, N. Jiménez, F. Alzate, G. Ruiz, D. Gutiérrez, S. Robledo, *J. Ethnopharmacol.* **2007**, *111*, 630–635.
[41] W. S. Koko, M. A. Mesaik, S. Yousaf, M. Galal, M. I. Choudhary, *J. Ethnopharmacol.* **2008**, *118*, 26–34.
[42] Molecular Operating Environment (MOE), 2014.09; Chemical Computing Group Inc., 1010 Sherbooke St. West, Suite #910,. Montreal, QC, Canada, H3 A 2R7, 2014.
[43] M. Naïm, S. Bhat, K. N. Rankin, S. Dennis, S. F. Chowdhury, I. Siddiqi, P. Drabik, T. Sulea, C. I. Bayly, A. Jakalian, E. O. Purisima, *J. Chem. Inf. Model.* **2007**, *47*, 122–133.
[44] I. Daoud, N. Melkemi, T. Salah, S. Ghalem, *Comput. Biol. Chem.* **2018**, *74*, 304–326.
[45] A. Toumi, S. Boudriga, K. Hamden, I. Daoud, M. Askri, A. Soldera, J. F. Lohier, C. Strohmann, L. Brieger, M. Knorr, *J. Org. Chem.* **2021**, *86*, 13420–13445.
[46] I. Daoud, F. Mesli, N. Melkemi, S. Ghalem, T. Salah, *J. Biomol. Struct. Dyn.* **2021**, doi:10.1080/07391102.2021.1973563.

Manuscript received: March 6, 2023
Revised manuscript received: March 30, 2023
Accepted manuscript online: April 6, 2023
Version of record online: April 20, 2023